

# Investigation on dynamic behavior of railway track in transition zone<sup>†</sup>

Jabbar-Ali Zakeri\* and Vida Ghorbani

Assistant Professor, School of Railway Engineering, Iran University of Science and Technology, Tehran, 16846-13114, Narmak, Iran

(Manuscript Received April 4, 2010; Revised August 14, 2010; Accepted October 24, 2010)

## Abstract

Railway track transition zone is a zone where track stiffness changes abruptly. This change occurs where the slab track connects to a conventional ballasted track, at the abutments of open-deck bridges, at the beginnings and ends of tunnels, at road and railway level crossings, and at locations where rigid culverts are placed close to the bottom of sleepers. In this paper, ballasted and slab tracks are simulated by two-dimensional model with two-layer masses. The transition zone is divided into three segments, each having a length of 6 meters with different specification and stiffness. The model of track consists of a Timoshenko beam as a rail and slab, lumped mass as sleepers, and spring and damper as ballast, sub-grade, and rail pad. The results of the dynamic analysis are presented and compared in two circumstances – one considering the transition zone and the other its absence.

*Keywords:* Transition zone; Dynamic behavior; Railway track; Rail pad; Track vertical stiffness

## 1. Introduction

In the design and construction of above-ground and under-ground railways, we sometimes face situations wherein track stiffness changes abruptly. It usually occurs where the slab track connects to a conventional ballasted track, at abutments of open-deck bridges, at road and railway grade crossings, and at the beginnings and ends of tunnels. In these regions, the design and construction of special superstructure is necessary. The purpose of transition zone is to bring a gradual adjustment between the subgrade modulus of the slab track and the ballasted track. Track reaction to wheel force is related to track stiffness and other factors. During train movement onto two tracks with different stiffness, there will be an abrupt change in response to existing track in the connection area [1].

One track problem is the severe change in vertical stiffness. In the transition zone, the vertical level of running wheel changes due to variations in track vertical stiffness. This change in elevation causes vertical acceleration imposition on running coach. Variable accelerations cause vertical dynamic load to change. The level of variations depends on the vertical displacement of rail in both sides of the transition zone, train speed, track modulus variations, and other factors. The sudden change in track vertical stiffness leads to uneven deflection, which causes abrupt change in the vertical level of the vehi-

cle's wheels. This change in elevation will excite the train component, i.e., the wheels, bogies, and coach, which in turn leads to vertical train-track interaction forces that are dynamically amplified in the transition zone [2].

Several studies have been performed about this subject on the design and construction of transition zone [3] and the study on the dynamic forces near bridge abutments [4, 5].

## 2. Design of transition zone

Different structural designs have been introduced and applied for transition zones [6]. One common design involves reducing the ballast layer thickness and applying concrete slab beneath the layer. In this research, the thickness of ballast layer is reduced in three steps from 30 to 20, then to 15, and finally to 0 centimeters. This design has been conducted in the entrance of one of the Bafgh-Mashhad railway tunnels in Iran.

As shown in Fig. 1, the length of each section is 6 meters and the slab thickness is reduced from 40 to 30 and then to 20 centimeters. Considering the common distance between fasteners, 60 cm, each section of the slab is modeled by 10 elements and 11 nodes. Consequently, the transition zone consists of 30 elements and 31 nodes (with 2 common nodes).

## 3. Modeling of railway track

The objective of this paper is to investigate the dynamic behavior of the transition zone. Accordingly, in order to compare the behavior of the transition zone with the ballasted and slab tracks, a 54 meter long track is simulated, in which

<sup>†</sup> This paper was recommended for publication in revised form by Editor Yeon June Kang

\*Corresponding author. Tel.: +98 9121053379, Fax.: +98 21 77451568

E-mail address: zakeri@iust.ac.ir

© KSME & Springer 2011

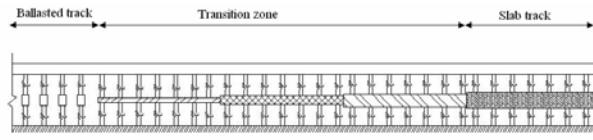


Fig. 1. Track modelling with two layers of masses.

the first 18 meters is the ballasted track, the middle 18 meters is the transition zone – which is modeled by the slab track with variation in vertical stiffness along the rail – and the last 18 meters is the slab track.

In modeling, two kinds of track structures are investigated as follows:

(1) Traditional ballasted track consisting of rail, sleepers, railpad, and elastic ballasted subgrade

(2) Slab track consisting of rail, railpad, and concrete slab placed on elastic subgrade

For the dynamic analysis, the longitudinal section of the ballasted track is simulated as two-layer masses on discrete supports, the rail as a beam, and sleepers as lumped masses. The slab track is modeled as two beams on discrete supports. This indicates that the only difference between the modeling of ballasted track and the slab track is that in the former, the lower layer, which is the sleeper, is modeled as a lumped mass, whereas the lower layer of the latter, which is the concrete slab, is simulated as a beam with bending stiffness. In this analysis, half of the track is simulated in two dimensions because of the symmetry of the track's sections [7, 8]. In the analysis of ballasted and slab tracks, the supports of the rail are considered as nodes and the length of the elements is 0.6 meters.

To obtain a gradual change in the vertical stiffness in the transition zone, the zone is divided into three 6-meter segments. The stiffness and damping of the railpad and the subgrade increases step by step from the value in the ballasted track to that in the slab track. Moreover, the slab's moment of inertia increases step by step. Therefore, the thickness of the slab must increase step by step.

The model length can exceed or, as in previous studies [9], the infinite boundary elements can be used to reduce the effects of the boundary conditions both in the ballasted and slab track models. The infinite boundary elements have been applied in this study. Therefore, the boundary conditions have no effect on the results [10].

#### 4. Modeling of the vehicle and wheel-rail contact

The vehicle has been considered to have 10 degrees of freedom – 2 degrees for the body, 2 degrees for each bogie, and 1 degree for each wheel. The vehicle is modeled by two four-axle bogies; the equations of motions are explained in our previous study [11]. Moreover, the wheel-rail contact is modeled by linearized Hertzian contact and the relation between the rail and the wheel movement is considered as follows:

$$F_w = C_H Z^{3/2} \quad (1)$$

$$k_H = \frac{dF}{dZ} = \frac{3}{2} C_H^{2/3} F^{1/3} \quad (2)$$

$$F_w = k_H [Z_w - v_r - R(x)] \quad (3)$$

where  $R(x)$  refers to the irregularities of the rail surface. Because of the investigation of the track behavior in the transition zone, rail corrugations have been neglected.

#### 5. Formation of track motion's equations matrix and solving it

The equation sets of the complete system motion are obtained by assembling the equations of motion with regard to each component of the track. The total equation is as follows:

$$[m]\{\ddot{Z}\} + [C]\{\dot{Z}\} + [K]\{Z\} = \{P(t)\} \quad (4)$$

where  $[m]$ ,  $[C]$ , and  $[K]$  are the mass, damping, and stiffness matrices of the system, respectively, which can be obtained by putting the matrix of each component in the relevant place of the total matrix.

In order to obtain the mass matrix of the rail, each element is assumed to be a beam segment consisting of nodes at the beginning and the end of the element. Each node has two degrees of freedom – vertical displacement and rotation of the perpendicular axis to the plane. The mass of each element of the rail is obtained by consistent mass matrix. Hence, the mass and stiffness matrices of the rail elements are expressed as follows:

$$M_r = \frac{\bar{m}L}{420} \begin{bmatrix} 156 & 22L & 54 & -13L \\ 22L & 4L^2 & 13L & -3L^2 \\ 54 & 13L & 156 & -22L \\ -13L & -3L^2 & -22L & 4L^2 \end{bmatrix} \quad (5)$$

$$K_r = \frac{2EI}{L^3} \begin{bmatrix} 6 & 3L & -6 & 3L \\ 3L & 2L^2 & -3L & L^2 \\ -6 & -3L & 6 & -3L \\ 3L & L^2 & -3L & 2L^2 \end{bmatrix} \quad (6)$$

where  $\bar{m}$  is the rail mass per unit length,  $L$  is the length of element,  $E$  is the modulus of rail, and  $I$  is the moment of inertia of the rail. The mass and stiffness matrices of the complete rail are obtained by assembling each element's matrix. The damping matrix of rail is obtained by Eq. (5):

$$[C_r] = \alpha [M_r] + \beta [K_r]. \quad (7)$$

Sleepers are modeled as lumped masses. Hence, the mass, stiffness, and damping matrices of sleepers are as follows:

$$[M_s] = \frac{M_s}{2} \begin{bmatrix} 1 & 0 & 0 & \dots & \dots & \dots & 0 \\ 0 & 1 & & & & & 0 \\ 0 & & 1 & & & & \\ \vdots & & & \ddots & & & \\ \vdots & & & & \ddots & & \\ \vdots & & & & & \ddots & \\ 0 & 0 & \dots & \dots & \dots & \dots & 1 \end{bmatrix} \quad (8)$$

$$[C_p] = C_p \begin{bmatrix} 1 & 0 & 0 & \dots & \dots & \dots & 0 \\ 0 & 1 & & & & & 0 \\ 0 & & 1 & & & & \\ \vdots & & & \ddots & & & \\ \vdots & & & & \ddots & & \\ \vdots & & & & & \ddots & \\ 0 & 0 & \dots & \dots & \dots & \dots & 1 \end{bmatrix} \quad (9)$$

$$[K_p] = K_p \begin{bmatrix} 1 & 0 & 0 & \dots & \dots & \dots & 0 \\ 0 & 1 & & & & & 0 \\ 0 & & 1 & & & & \\ \vdots & & & \ddots & & & \\ \vdots & & & & \ddots & & \\ \vdots & & & & & \ddots & \\ 0 & 0 & \dots & \dots & \dots & \dots & 1 \end{bmatrix} \quad (10)$$

Thus, the motion equation of sleepers is given by the following:

$$[M_s][\ddot{Z}_s] + [C_p][\dot{Z}_s(t) - \dot{Z}_r(x,t)] + [C_B][\dot{Z}_s] + [K_p][Z_s(t) - Z_r(x,t)] + [K_B][Z_s] = 0 \quad (11)$$

where  $K_p$  and  $K_B$  are the stiffness of the railpad and ballast,  $C_p$  and  $C_B$  are the damping of the railpad and ballast, and  $Z_r(x,t)$  and  $Z_s(t)$  are the vertical displacement of the rail and sleeper in time (t), respectively.

Each element of concrete slab is modeled as a Timoshenko beam where  $\bar{m}$  is the slab mass per unit length, k is th stiffness matrix of ij element (see Eq. (10)), E is the modulus of the slab, and I is the moment of inertia of the slab.

$$k_{ij} = \begin{bmatrix} \alpha & -\alpha & \beta & \beta \\ -\alpha & \alpha & -\beta & -\beta \\ \beta & -\beta & \gamma & \rho \\ \beta & -\beta & \rho & \gamma \end{bmatrix}, \begin{matrix} \alpha = \frac{12EI_z}{l^3(1+s_y)} \\ \beta = -\frac{6EI_z}{l^2(1+s_y)} \\ \gamma = \frac{(4+s_y)EI_z}{l(1+s_y)} \\ \rho = \frac{(2-s_y)EI_z}{l(1+s_y)} \end{matrix}, s_y = \frac{12EI_z}{l^2(GA_y)} \quad (12)$$

Table 1. Material properties of railway track components.

Component track		Mass [kg/m]	Stiffness [kN/m]	Damping [kN.S/m]
Ballasted track	Rail (UIC60)	60	-	-
	Railpad	-	200 × 103	28
	Sleeper	320	-	-
	Ballast	-	46 × 103	180
Slab track	Railpad	-	375 × 103	135
	Slab	1876	-	-
	subgrade	-	60 × 103	180

In the calculation, the vehicle with two bogies and four wheels are considered to transit on the track. It is assumed that in the primary step, the first wheel is placed on the first node. In the next step, after a period of time ( $\Delta t$ ), the wheel moves forward. In terms of vehicle speed, if the wheel is placed on the node, one array of the stiffness matrix obtains value from the force vector, whereas if it is placed on the beam element, four arrays of stiffness matrix get value. In order to solve the differential equation and to attain results, the Newmark numerical method has been applied [11].

Table 1 shows the dynamic specifications of track components. As can be seen from the table [6], the respective values of stiffness and damping of the railpad are  $243.75 \times 10^3$  kN/m and 54.75 kNs/m in the first 6 meters of the transition zone;  $287.5 \times 10^3$  kN/m and 81.5 kNs/m in the mid 6 meters of the transition zone; and  $331.25 \times 10^3$  kN/m and 108.25 kNs/m in the last 6 meters of the transition zone.

**6. Comparison of Track Dynamic Behavior: Assuming Transition Zone Existence and Absence**

The results of maximum displacement, acceleration, and vibrational velocity have been discussed in two cases, one assuming the transition zone and the other its absence.

To obtain a maximum displacement graph, the value of the maximum displacement in the time history of the relevant node should be calculated. Fig. 2, plotted in the absence of transition zone, shows the displacement variation in a length that is less than 2 m to reach its maximum, and displacement varies from 1.17 to 0.7 mm. Therefore, the acceleration varies suddenly in a short length and causes the track to oscillate, which can cause destructive effects. However, according to Fig. 3, provided the transition zone exists, the displacement difference occurs step by step in three stages along 18 meters.

According to Fig. 4, in the connection point of the ballasted track and the slab track, the maximum vertical acceleration increased abruptly from 6.6 m/s<sup>2</sup> to 8 m/s<sup>2</sup>, thus there is a variation in rail acceleration of about 1.4 m/s<sup>2</sup>. In the slab track part, vibrational acceleration rises from 3.1 m/s<sup>2</sup> up to 3.6 m/s<sup>2</sup>. This means that there is 21% increase in acceleration in the ballasted part and 16% in the slab track.

Fig. 5 indicates that the difference in oscillation is largest from the ballasted track to the first part of the transition zone.

To state the matter differently, the vibrational acceleration

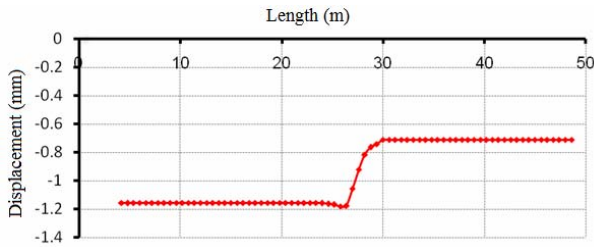


Fig. 2. Maximum displacement of rail in the absence of transition zone.

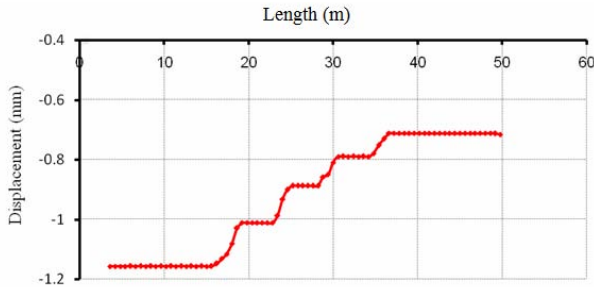


Fig. 3. Maximum displacement of rail assuming the existence of transition zone.

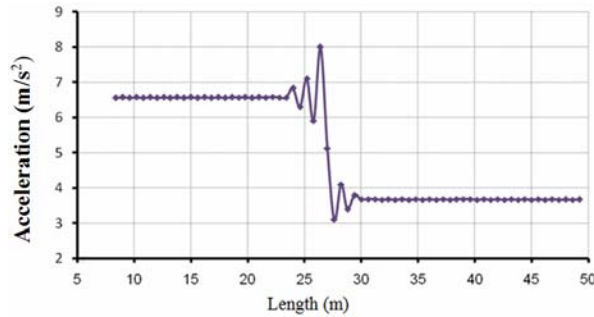


Fig. 4. Maximum acceleration of rail in the absence of transition zone.

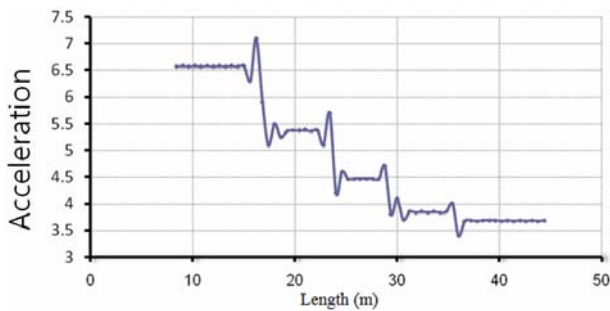


Fig. 5. Maximum acceleration of rail assuming the existence of transition zone.

increased 7.5% from  $6.6 \text{ m/s}^2$  to  $7.1 \text{ m/s}^2$ . The increase clearly decreased (from 21% to 7.5%), which indicates the importance of the transition zone. Moreover, the acceleration values in the four stages did not decrease similarly. Thus, the relation between acceleration and stiffness changes is not linear.

According to Fig. 6, the railpad force in the ballasted track increased from around 42 kN to 70 kN in the slab track. Railpad force depends on two factors: (1) the elevation

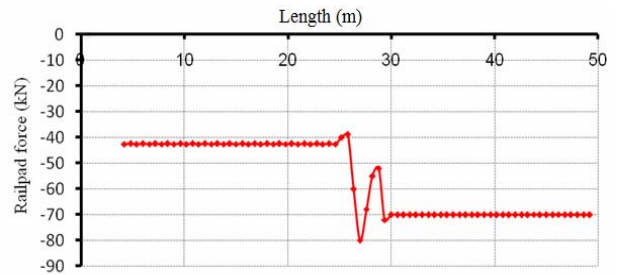


Fig. 6. Maximum railpad force in the absence of transition zone.

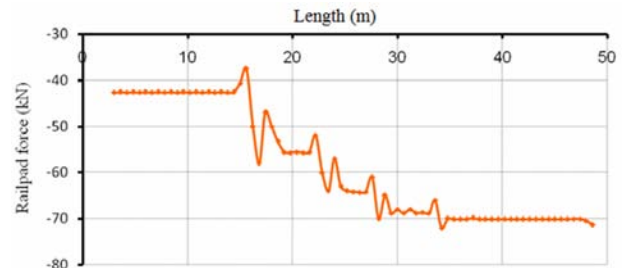


Fig. 7. Maximum railpad force assuming the existence of transition zone.

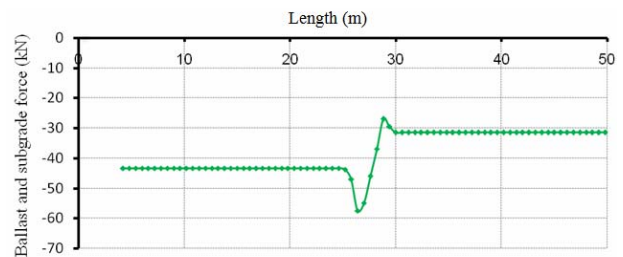


Fig. 8. Maximum force of ballast and subgrade in the absence of transition zone.

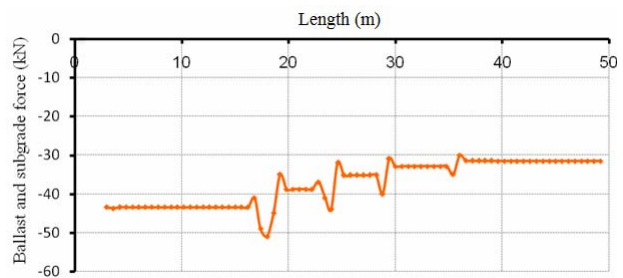


Fig. 9. Maximum force of ballast and subgrade assuming the existence of transition zone.

difference between rail and sleeper in the ballasted track and between the rail and slab in the slab track, and (2) the stiffness of the railpad.

The stiffness of the railpad is 200 MN/m in the ballasted track and 375 MN/m in the slab track. Thus, the trend of the railpad force changes in track is not discussed. What is important is the abrupt increase in the force of railpad in the ballasted track and slab track connection. According to Fig. 6, in a short period of time and along a short length, the force

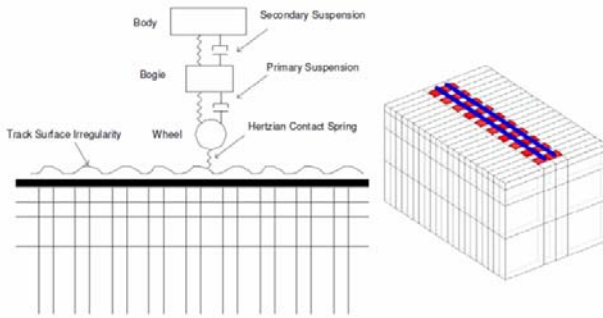


Fig. 10. Schematic layout of three-dimensional coupled track-train model.

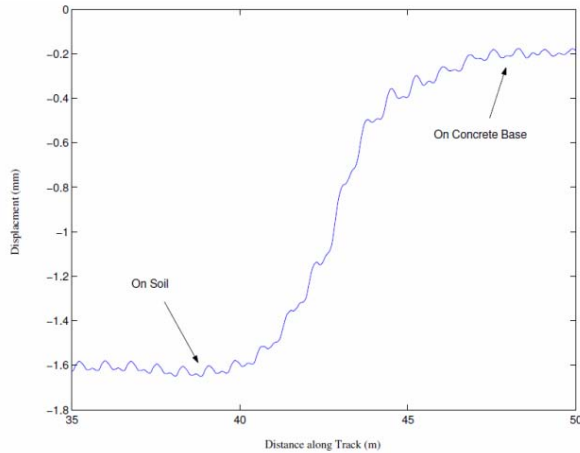


Fig. 11. Rail displacement in a stiffness transition under wheel load.

increased from 40 kN to 80 kN, which can have harmful effects.

In Fig. 7, the railpad force in the ballasted track reaches 58 kN from 42 kN, showing an increase of 38%. This means that the transition zone causes the force increase to drop by 52%.

Fig. 8 shows the force in the ballast and subgrade. As can be seen, the ballast force is approximately 43 kN and the force of subgrade is 31 kN. Furthermore, the force increases from 43 kN to 58 kN in the mid length, showing a 35% increase in the force, which is less than the force change in the railpad.

In Fig. 9, the ballast force increases 18% from 43 kN to 51 kN due to the track's structure change, indicating that the transition zone caused the increase in force to drop 50%.

## 7. Results validation

To show the validity of the mathematical model of mechanical systems, two methods must be done: applying field studies or using the results of previous studies that have been confirmed. Control of displacements or vibrational accelerations of vehicles and rail can be applied for the confirmation of the model. Considering existing data, the displacement control has been applied in this paper.

For more comparison and investigation about the attained results, we refer to the results of Banimahd's work [12],

wherein a three-dimensional finite element model was applied to study the mechanics of railway track transitions (Fig. 10). The applied model incorporates the multi-layered nature of the sub-structure, soil, and ballast nonlinearity and the interaction between the track and train. The model of the track consists of rail, railpad, sleeper, ballast, sub-ballast, and several subgrade layers. The effect of transition length and train speed on the track–train performance has been investigated in terms of the rail wheel interaction force and the train body acceleration [6].

Fig. 11 shows rail displacement in the transition zone under wheel loading without any void under the sleepers and no geometric irregularity in the rail or track substructure. As shown in the figure, when the stiffness change varies gradually, displacement also varies gradually. This is the reason for transition zone execution [4].

Moreover, the results of Refs. [13] and [6] can be used for comparison.

## 8. Conclusion

The results of track modeling in MATLAB software shows vertical displacement difference and rail acceleration, and velocity difference in the ballasted track and transition zone connection is greater in the slab track and transition zone connection. In the absence of transition zone, the displacement difference reaches its peak, causing the sudden variation in acceleration in a short period and the oscillation of the track. However, in the case where the transition zone is considered, variations will be distributed along the transition zone and moderates the shock. The vertical acceleration of rail, sleepers, and slab shows that acceleration change in the rail is greater than that of sleeper and slab. In the connection area of ballasted track to slab track, the acceleration changes noticeably.

The trend of the railpad force changing from the ballasted track to the slab track cannot be obtained, but what is important is the sudden increase of railpad force in the ballasted track and slab track connection. This condition also applies to the ballast force when the variations are less than the railpad force, which can be resolved considering the transition zone.

## References

- [1] A. D. Kerr, *Fundamentals of Railway Track Engineering*, Simmons-Boardman Books, Inc. (2003).
- [2] C. Esveld, *Modern Railway Track*, Second edition, TU-Delft (2001).
- [3] H. R. Lotfi and R. G. Oesterle, *Slab track for 39-ton loads, structural design*, R&D SN2832, Portland, Cement Association, Skokie, Illinois, USA (2005).
- [4] H. E. M. Hunt Settlement of railway track near bridge abutments, *Proc. Instn. Civ. Engrs, Transp.* (1997) 68-73.
- [5] D. Li and D. Read, *Research results digest 79*, Transportation Technology Center, Inc.(TTCI), (2006).
- [6] V. Ghorbani, *Investigation of dynamic behavior of super-structure track railway in transition zone*. MSc. Thesis, Iran

- University of Science and Technology (2009).
- [7] M. Ishida and T. Suzuki, Effect on track settlement of interaction excited by leading and trailing axles, *QR of RTRI*, 64 (1) (2005).
- [8] D. Younesian and M. H. Kargarnovin, Response of the beams on random Pasternak foundations subjected to harmonic moving loads, *Journal of Mechanical Science and Technology*, 23 (11) (2009) 3013-3023.
- [9] J. A. Zakeri and H. Xia, Application of 2D-infinite beam elements in dynamic analysis of railway track, *Journal of Mechanical Science and Technology*, 23 (5) (2009) 1415-1421.
- [10] J. A. Zakeri, J. J. Fan, H. Xia, Dynamic Responses of Train –Track system to Single Rail Irregularity, *Latin American Journal of Solids and Structures*, 6 (2) (2009) 89-104.
- [11] J. A. Zakeri and H. Xia, Sensitivity Analysis of Track Parameters on Train- Track Dynamic Interaction, *Journal of Mechanical Science and Technology*, 22 (7) (2008) 1299-1304.
- [12] M. Banimahd, P. K. Woodward, 3-Dimensional finite

element modeling of railway transitions, XiTRACK, *Proceedings 9th International Conference on railway engineering London* (2007).

- [13] *Bridge approaches and track stiffness*, U.S. Department of transportation, Federal Railroad Administration, April 2007.



**Jabbar Ali Zakeri** received his B.S. degree in Civil Engineering and M.Sc. degree in Structural Engineering from Tabriz University in 1992 and 1995, respectively. He then went on to receive his Ph.D. degree in Road and Railway Engineering from Beijing Jiaotong University in 2000. Dr. Zakeri

is currently an Assistant Professor at the School of Railway Engineering at Iran University of Science and Technology. His research interests are in the area of dynamic analysis of train – track interaction, railway track dynamics, track maintenance, and construction.